Transcription factor-7-like 2 (TCF7L2) gene acts downstream of the Lkb1/Stk11 kinase to control mTOR signaling, β cell growth, and insulin secretion

Nguyen-Tu, Marie-Sophie; da Silva Xavier, Gabriela; Leclerc, Isabelle; Rutter, Guy A

DOI:
10.1074/jbc.RA118.003613

Document Version
Peer reviewed version

Citation for published version (Harvard):
Nguyen-Tu, M-S, da Silva Xavier, G, Leclerc, I & Rutter, GA 2018, 'Transcription factor-7-like 2 (*TCF7L2*) gene acts downstream of the *Lkb1/Stk11* kinase to control mTOR signaling, β cell growth, and insulin secretion', *Journal of Biological Chemistry*. https://doi.org/10.1074/jbc.RA118.003613

Transcription factor-7-like 2 (*TCF7L2*) gene acts downstream of the *Lkb1/Stk11* kinase to control mTOR signaling, β cell growth, and insulin secretion

Marie-Sophie Nguyen-Tu, Gabriela da Silva Xavier, Isabelle Leclerc, and Guy A. Rutter*

Section of Cell Biology and Functional Genomics, and Pancreatic Islet and Diabetes Consortium, Division of Diabetes, Endocrinology and Metabolism, Imperial Centre for Translational and Experimental Medicine, Department of Medicine, Imperial College London, London W12 0NN, UK

Running title: *Lkb1* regulates *Tcf7l2* action in β cells

*Address correspondence to Professor Guy A. Rutter, Imperial College London, Hammersmith Hospital campus, DuCane road W12 0NN London, UK;
Tel: +44 020759 43351
email: g.rutter@imperial.ac.uk

Keywords: Pancreatic β cell; insulin secretion; cell growth; TCF7L2; LKB1

ABSTRACT

Variants in the transcription factor-7-like 2 (*TCF7L2/TCF4*) gene, involved in Wnt signaling, are associated with type 2 diabetes. Loss of *Tcf7l2* selectively from the β cell in mice has previously been shown to cause glucose intolerance and to lower β cell mass. Deletion of the tumour suppressor liver kinase B1 (LKB1/STK11) leads to β cell hyperplasia and enhanced glucose-stimulated insulin secretion, providing a convenient genetic model for increased β cell growth and function. The aim of this study was to explore the possibility that *Tcf7l2* may be required for the effects of *Lkb1* deletion on insulin secretion in the mouse β cell. Mice bearing *floxed Lkb*1 and/or *Tcf7l2* alleles were bred with knock-in mice bearing *Cre* recombinase inserted at the *Ins1* locus (Ins1Cre), allowing highly β cell-selective deletion of either or both genes. Oral glucose tolerance was unchanged by the further deletion of a single *Tcf7l2* allele in these cells. By contrast, mice lacking both *Tcf7l2* alleles on this background showed improved oral glucose tolerance and insulin secretion *in vivo* and *in vitro* compared to mice lacking a single *Tcf7l2* allele. Bi-allelic *Tcf7l2* deletion also enhanced β cell proliferation, increased β cell mass and caused changes in polarity as revealed by the "rosette-like" arrangement of β cells. *Tcf7l2* deletion also increased signaling by Target of Rapamycin (mTOR), augmenting phospho-ribosomal S6 levels. We identified a novel signaling mechanism through which a modifier gene, *Tcf7l2*, lies on a pathway through which LKB1 acts in the β cell to restrict insulin secretion.

Type 2 diabetes currently affects 415 million individuals worldwide and this number is expected to rise to >600 million by 2040 (www.diabetesatlas.org). Pancreatic β cell failure is an essential, if still poorly understood, component of disease development and progression (1).

Genome-wide association studies (GWAS) have identified more than 100 *loci* associated with disease risk (2), with the majority affecting insulin secretion rather than the action of the hormone. Although in a few cases the likely effector transcript has been identified (3,4), for most *loci* neither the causal gene, nor its mechanism of action at the cellular level, has been

defined. Of the commonly inherited risk variants, those in the T-cell factor 7–like-2 (*TCF7L2/TCF4*) gene, including rs7903146, display amongst the highest odds ratio for exaggerated type 2 diabetes risk (~1.2/allele) (5). The identified single nucleotide polymorphism (SNP) rs7903146 is located in the third intron of TCF7L2 and has been estimated to contribute to 10-25% of all cases of diabetes lean patients (6) TCF7L2 lies at the foot of the wingless (Wnt) signaling pathway activated both by Wnt ligands and by certain growth factors (e.g. insulin, IGF-1) which act through receptor tyrosine kinases (7). In the presence of Wnt ligands, a signaling cascade results in stabilization and nuclear localization of β-catenin, which interacts with T cell-specific factor/lymphoid enhancer-binding factor (TCF/LEF) to control transcription of target genes. In the absence of Wnt ligands, β-catenin is degraded by protein complexes including axin-2 and glycogen synthase kinase 3β (GSK-3β) (8).

Several studies have explored the role of *Tcf7l2* in insulin secretion in model systems. Thus, inhibition of TCF7L2 activity in human or in rat insulinoma cell line (9,10) inhibited insulin secretion in response to glucose. Likewise, deletion of the *Tcf7l2* gene selectively in the β cell in mice (11,12) reduced insulin production in older animals and impaired the expansion of β cell mass in response to a high fat diet (11,12). Finally, in a separate study (13), re-expression of TCF7L2 on a null background improved glucose tolerance. Importantly, the degree to which the action of disease risk variants on the β cell may be context-dependent is unclear. Thus, TCF7L2 variants could have different patho-physiological effects among the five different subpopulations of diabetic patients identified in a recent study (14). The mechanisms, including the genetic drivers, behind these differences remain obscure.

Here, we have explored the impact of *Tcf7l2* deletion in a model of β cell expansion driven by artificially enhanced growth factor signaling. Several earlier observations have suggested that a reciprocal relationship may exist between the tumour suppressor Liver Kinase B1 LKB1/STK11 (LKB1) and TCF7L2 signaling in other systems. Firstly, the LKB1/STK11 homologue XEEK1 is required for Wnt signaling in Xenopus laevis, and acts by phosphorylating and inactivating glycogen synthase kinase-3 (GSK3) (40). Moreover, in Peutz-Jeghers syndrome, Wnt signaling activation is correlated to LKB1 expression (41). Similarly, in oesophageal carcinoma patients, LKB1 is down-regulated while Wnt target genes are up-regulated through inhibition of GSK3β activity (42). We (15,16), and others (17,18), have shown previously that inactivation of LKB1, in the β cell leads to a substantial increase in insulin production and improved glucose tolerance. LKB1 is a tumour suppressor mutated in Peutz-Jeghers syndrome, a premalignant condition characterised by hamartomatous polyps and an increased risk of all cancers (19,20). Although the mechanisms involved remain to be fully elucidated, increases in β cell mass (15), changes in the signaling pathways activated by glucose (16,21), and alterations in cellular morphology and polarity (15,17,18) all appear to play a role in enhancing insulin secretion in the *Lkb1*-null β cell. Acting via the fuel-sensitive enzyme AMP-activated protein kinase (AMPK), and the Tuberous Sclerosis Complex TSC1-TSC2, LKB1 also inhibits mammalian target of rapamycin (mTOR) signaling to restrict protein synthesis and cell division (22). This pathway may oppose β cell expansion in the adult, since AMPK is likely to be active in these cells in the fasting state (23,24).

To explore the above possibilities, we have used an epistasis approach to examine the impact on the pancreatic β cell of deleting *Tcf7l2* in the absence of *Lkb1* alleles. We show that, in contrast to the action of *Tcf7l2* ablation to impair insulin secretion in wild-type mice, loss of this transcription factor on an *Lkb1* null background further increases insulin secretion, β cell size, β cell mass, and augments mTOR activity, consistent with a role for TCF7L2 as an inhibitor of mTOR signaling.

Results

Generation of β cell specific Lkb1/Tcf7l2 double knockout mice

To study the impact of the deletion of *Tcf7l2* and *Lkb1* in the pancreatic β cell, we established breeding pairs on a mixed background (C57BL/6J, FVB/NJ and 129sS1/SvlmJ) to produce offspring deleted for *Lkb1* and / or *Tcf7l2* selectively in the β cell using the highly selective *Cre* deleter strain *Ins1Cre* in which *Cre* recombinase is inserted into the *Ins1* locus (25,26) (Figure 1A and B). Deletion at other sites, including the brain, is minimal in this model and, importantly, the transgene does not carry the human growth hormone minigene present in alternative *Cre* strains (e.g. RIP2.Cre) (27). Consequently, effects of *Ins1Cre* expression alone on glucose homeostasis are not observed. Since a strategy generating all possible genotypes would have produced mice homozygous for deletion of both alleles at a frequency of 1 per 64 pups, we designed instead two-separate breeding colonies to reduce animal numbers, in accordance with the 3Rs. The following offspring were produced and named as follow (group 1): control (*Ins1Cre*$^{-/-}$*:Lkb1*$^{f/f}$*:Tcf7l2*$^{f/+}$), βLkb1-KO (*Ins1Cre*$^{+/-}$*:Lkb1*$^{f/f}$*:Tcf7l2*$^{+/+}$), and βLkb1-KO-Tcf7l2-het (*Ins1Cre*$^{+/-}$*:Lkb1*$^{f/f}$*:Tcf7l2*$^{f/+}$; Figure 1A). The second breeding strategy (group 2) generated littermates βLkb1-KO-Tcf7l2-het (*Ins1Cre*$^{+/-}$*:Lkb1*$^{f/f}$*:Tcf7l2*$^{f/+}$) and βLkb1-Tcf7l2-dKO (*Ins1Cre* $^{+/-}$*: Lkb1*$^{f/f}$*:Tcf7l2*$^{f/f}$; group 2, Figure 1B).

We first measured *Lkb1* and *Tcf7l2* gene expression in isolated islets using RT-qPCR analysis. The level of endogenous *Lkb1* mRNA was strongly decreased in the presence of *Cre* transgene when one single or both *Tcf7l2* alleles were *floxed*, as expected. Likewise, the level of *Tcf7l2* mRNA was decreased when both alleles were *floxed* (βLkb1-Tcf7l2-dKO) compared to control. Importantly, we observed no significant differences in the level of *Lkb1* and *Tcf7l2* mRNA between βLkb1-KO-Tcf7l2-het mice from either group 1 or 2. Of note, deletion of *Lkb1* significantly increased *Tcf7l2* expression when both *Tcf7l2* alleles were present in βLkb1-KO mice (Figure 1C and D). Likewise, we observed decreased LKB1 and TCF7L2 protein expression in isolated islets from βLkb1-KO, βLkb1-KO-Tcf7l2-het and βLkb1-Tcf7l2-dKO compared to control islets (Figure 1E).

Deletion in the β cell of two Tcf7l2 alleles in an Lkb1 null background improves oral glucose tolerance and insulin secretion

Consistent with previous findings (15-18,25), deletion of both *Lkb1* alleles in the β cell improved glucose tolerance in mice aged 8 weeks (Figure 2A, B). These changes were not associated with any alteration in body weight (Figure S1A). Glucose tolerance was not further affected by the additional deletion of a single *Tcf7l2* allele (Figure 2A, B). Deletion of *Lkb1* alone also lowered fed glycemia, and this action was attenuated by the additional deletion of *Tcf7l2* (Figure S1B). Insulin sensitivity was unchanged by deletion of a single *Tcf7l2* allele (Figure S1D).

As previously described (15-18,25), *Lkb1* deletion substantially increased insulin release in response to glucose *in vivo* (Figure 2C). Interestingly, glucose-stimulated insulin secretion *in vitro* only tended to increase on an *Lkb1* null background compared to control (Figure 2D). Mono-allelic *Tcf7l2* deletion had little further impact on these changes such that the glycemic phenotype of βLkb1-KO-Tcf7l2-het did not differ from βLkb1-KO mice *in vivo*, but insulin release was enhanced *in vitro* (Figure 2C and D). In contrast, when βLkb1-KO-Tcf7l2-het mice were compared to homozygous βLkb1-Tcf7l2-dKO animals deleted for both *Tcf7l2* alleles we observed a further improvement in glucose tolerance (Figure 3A, B), but unchanged, body weight, fed glycemia and insulin sensitivity (Figure S2A, C, E). A substantial (~2-fold) increase in acute insulin release in response to glucose injection was also observed *in vivo* (Figure 3C, D) when comparing βLkb1-Tcf7l2-dKO with

βLkb1-KO-Tcf7l2-het littermates. Likewise, comparing islets isolated from mice deleted for both *versus* a single *Tcf7l2* allele, insulin secretion was significantly increased in response to elevated glucose but not to depolarisation with KCl (Figure 3E). Thus, deletion of *Tcf7l2* on a *Lkb1* null background exerts an effect whose direction is opposite to that seen in control islets (11,12). In females, deletion of one or two *Tcf7l2* alleles on a *Lkb1* null background did not affect oral glucose tolerance, insulin sensitivity, fed glycemia and body weight compared to *Lkb1* deletion only (βLkb1-KO; Supplemental Figure S2).

Next, we sought to explore intracellular free calcium (Ca^{2+}) dynamics to elucidate whether these may be altered and contribute to the enhanced insulin secretion. Islets derived from βLkb1-KO mice displayed a delayed and decreased response to high glucose in free cytosolic Ca^{2+} increases compared to control animals (Figure 4A and B). A similar degree of impairment was observed after the additional deletion of a single *Tcf7l2* allele. Interestingly, islets from βLkb1-KO mice showed a decreased response to depolarisation with KCl compared to control mice, whereas βLkb1-KO-Tcf7l2-het islets displayed a similar response to KCl compared to control islets (Figure 4A and C). In group 2, no difference in response to high glucose or KCl was noted between islets from βLkb1-KO-Tcf7l2-het and βLkb1-Tcf7l2-dKO mice (Figure 4D, E and F).

Impact of Lkb1 and Tcf7l2 deletion on islet morphology

We next examined β cell size, and the distribution of β cells within the islet, in pancreatic slices (Figure 5A, B). Cellular proliferation was also assessed through Ki67 staining (Figure 5C). As previously reported (15-18,25), deletion of *Lkb1* increased the number of "rosette-like" structures within each islet, as identified using the adherens junction marker E-cadherin, likely reflecting a change in cellular polarity (Figure 6A, B) (see (15,18). The number of rosette structures was not significantly affected by deletion of a single *Tcf7l2* allele whilst the deletion of both alleles tended (p=0.055) to increase this number, a change which may also contribute to the enhanced secretion observed (15,18).

β Cell mass did not show any significant differences after *Lkb1* deletion, deletion of a single *Tcf7l2* allele had no further effect (Figure 6C). In contrast, deletion of both *Tcf7l2* alleles caused a substantial (>30%) and significant increase in β cell mass as examined in βLkb1-Tcf7l2-dKO *versus* βLkb1-KO-Tcf7l2-het littermates. Correspondingly, β cell proliferation, examined by Ki67 staining, was not affected by *Lkb1* deletion alone, nor the loss of a single *Tcf7l2* allele, but significantly increased when two *Tcf7l2* alleles were deleted (Figure 5C and Figure 6E, F). β cell size, as assessed by comparing islet volume to the number of DAPI-labelled nuclei/islet, was significantly increased by *Lkb1* deletion, but not further affected by either mono- or bi-allelic deletion of *Tcf7l2* (Figure 6 G, H).

Impact of Tcf7l2 deletion on mTOR signaling

As previously described (15,17), mTOR signaling is implicated in β cell hypertrophy when *Lkb1* is deleted. We therefore examined whether *Tcf7l2* deletion may impact mTOR signaling. Whereas deletion of *Lkb1* alone had no effect on the levels of phospho-ribosomal protein subunit S6 (rpS6) (Figure 7A, B, D), a significant increase was observed in βLkb1-Tcf7l2-dKO *vs* βLkb1-Tcf7l2-het islets by immunostaining of pancreatic slices (Figure 7A, C), and confirmed by Western (immuno-) blotting (Figure 7E).

Regulation of Wnt signaling

Finally, we explored the effects of LKB1 and TCF7L2 deletion on genes in the Wnt/β-catenin pathway. We found that β-catenin, the transcriptional activator for the TCF family of transcription factors, and axin-2, a negative loop regulator of Wnt signaling, tend to be downregulated in the absence of LKB1 (Figure 8A). However, axin-2 was upregulated by LKB1 and TCF7L2 deletion (Figure 8B).

Therefore, it is possible that a cross-talk exists between LKB1 and Wnt/TCF7L2 signaling in pancreatic islets and that this could be involved in controlling β cell proliferation. Furthermore, it is possible that Lkb1 could be a regulator of Wnt signaling and that TCF7L2 is involved for loop regulation of Wnt signaling involved in proliferative signaling induced by Wnt ligands.

Discussion

The overall aim of the present study was to determine whether, under conditions of exaggerated β cell proliferation, the role of *Tcf7l2* may differ from that previously described in animals placed under metabolic stress imposed by aging or by a high fat diet (11,12). To this end we used a mouse model in which *Lkb1* was deleted selectively in β cells mimicking, at least in part, changes during early development (28,29), pregnancy (30,31) or insulin resistance ("compensation") prior to the onset of type 2 diabetes (32,33). This has seemed an important question given that apparent differences in action have previously been described for other GWAS-identified type 2 diabetes genes, such as *SLC30A8* (34-36) when modelled in mice.

Strikingly, we demonstrate that the direction of the effect of *Tcf7l2* deletion is reversed under these conditions (β cell hyper-function) *versus* those seen under metabolic stress (11,12). Given that TCF7L2 is normally considered to be a positive regulator of the cell cycle, and thus pro-proliferative (37,38), this result was unexpected. We therefore considered carefully the possibility that this might be due to alterations elsewhere in the genome given that the *Lkb1* alleles (FVB/N/129S1) were carried by animals with a slightly different genetic background to the floxed *Tcfl72* strain (C57BL/6J) used (see Supplemental Table S1). Although this possibility cannot be excluded absolutely we believe it is unlikely given that both FVB/N (39) and 129S1 (40) animals display similar glucose tolerance on a regular chow diet to C57BL/6 mice.

As an alternative explanation, we speculated that *Tcf7l2* acts as a negative regulator of mTOR signaling. This view was supported by the data shown in Figure 7, which demonstrated increased mTOR signaling after deletion of both, but not a single, *Tcf7l2* allele. Interestingly, in the present study we saw relatively little effect of *Lkb1* deletion on mTOR signaling in the presence of *Tcf7l2*, despite the predicted activation of the downstream TCS1/TCS2 complex in the absence of AMPK activity (22). Nevertheless, and interestingly, loss of TCF7L2 impacted the alterations in β cell apical-basolateral polarity observed after *Lkb1* ablation (15-18,25), which lead to alterations in the number of “rosette” structures. The latter changes have previously been ascribed to alterations in signaling by the AMPK-related kinase MARK2/*Par1b* (18).

Interestingly, increased *Tcf7l2* and decreased *β-catenin* mRNA levels were also observed after *Lkb1* deletion in the present study, providing evidence for an interaction between these genes in the β cell wherein LKB1 represses *Tcf7l2* expression (Figure 8). Morever, we found that axin-2 was regulated positvely and negatively, respectively, by *Lkb1* and *Tcf7l2*.

We also noted that deletion of *Tcf7l2* on an *Lkb1* null background resulted both in changes in β cell growth (i.e. hypertrophy and hyperplasia) but also increased β cell function (secretion of insulin as normalized to total insulin content). While increased mTOR signaling provides a likely mechanism for the former, the mechanisms driving increased insulin secretion remain unclear. In recent studies, we (16) and others (21) demonstrated that loss of LKB1 signaling resulted in marked alterations in glucose signaling to ATP generation and calcium dynamics, such that the so-called "amplifying" pathway, of insulin secretion (41,42), possibly mediated by enhanced synthesis of glutamate and other amino acids, became the predominant means through which hormone release was activated in response to the sugar. The present study confirmed these findings (Figure 4A). Importantly,

we observed no evident improvement in Ca^{2+} dynamics in response to elevated glucose or KCl after deletion of a single or both *Tcf7l2* alleles. This observation argues against the view that *Tcf7l2* deletion leads to a reversion to a more conventional route for glucose-stimulated insulin secretion, chiefly reliant on the closure of ATP-dependent K^+ channels (43) and calcium influx. Instead, the new findings point towards a further enhancement of the amplifying pathways for insulin secretion in β cells lacking both *Tcf7l2* alleles in the absence of *Lkb1*.

The present data may also provide a mechanistic underpinning for other findings in the literature which have pointed to a possible interaction between nutrient levels and *TCF7L2* action. For example, the action of *TCF7L2* risk (T) allele rs7903146 was dependent on plasma glucose levels during oral glucose tolerance tests (44), with deleterious actions being most apparent at high glucose, and even tending to be protective at low glucose. We would note that although the direction of this effect might appear to be the reverse of that reported here in mice, the above study is likely chiefly to have interrogated the actions of incretins on insulin secretion, which were not examined here. Nevertheless, glucose-dependent suppression of AMPK activity, likely to mimic the effect of *Lkb1* deletion on mTOR activity, may provide a means through which changes in glycemia modulate the direction of effect of *TCF7L2* variants on type 2 diabetes risk.
In summary, we demonstrate here that *Tcf7l2* acts as a modifier gene for *Lkb1* in the β cell, affecting islet polarity, cellular proliferation and mass via mTOR signaling. These findings may be relevant for our understanding of the actions of human *TCF7L2* variants on type 2 diabetes risk in different individuals and settings (14).

Experimental procedures

Generation of mutant mice lacking LKB1 and TCF7L2 selectively in pancreatic β cells.

Mice homozygous for the floxed *Lkb1/Stk11* gene (mixed FVB/129S1 and C57BL/6 background) (15) were crossed to mice homozygous for floxed ($^{f/f}$) *Tcf7l2* alleles (C57BL/6 background) (12). The resulting double heterozygotes (*Lkb1*$^{f/+}$*:Tcf7l2*$^{f/+}$) were crossed with double heterozygous mice and the latter then bred with mice expressing *Cre* recombinase at the *Insulin 1* locus (*Ins1.Cre*) (25,26). Subsequently, two-separate breeding colonies were established to produce the following offspring, and named as follow (group 1): control (*Ins1Cre*$^{-/-}$*:Lkb1*$^{f/f}$*:Tcf7l2*$^{f/+}$), βLkb1-KO (*Ins1Cre*$^{+/-}$*:Lkb1*$^{f/f}$*:Tcf7l2*$^{+/+}$), and βLkb1-KO-Tcf7l2-het (*Ins1Cre*$^{+/-}$*:Lkb1*$^{f/f}$*:Tcf7l2*$^{f/+}$; Figure 1A). The second breeding strategy generated littermates βLkb1-KO-Tcf7l2-het (*Ins1Cre*$^{+/-}$*:Lkb1*$^{f/f}$*:Tcf7l2*$^{f/+}$) and βLkb1-Tcf7l2-dKO (*Ins1Cre*$^{+/-}$*:Lkb1*$^{f/f}$*:Tcf7l2*$^{f/f}$; group 2, Figure 1B). Genetic background of the resulting crosses was quantified by SNP genome scanning analysis (Jax® Laboratories; Table S1).

Mouse maintenance and diet

Animals were housed 2-5 per individually-ventilated cage in a pathogen-free facility with 12 h light/dark cycle and had free access to standard mouse chow diet. Unless otherwise stated, data presented are those obtained using male mice. All *in vivo* procedures described were performed at the Imperial College Central Biomedical Service and approved by the UK Home Office Animals Scientific Procedures Act, 1986 (HO Licence PPL PA03F7F07 to I.L.).

Measurement of metabolic parameters *in vivo*

Glucose tolerance was performed on 15 h-fasted mice after an oral gavage of glucose (2 g/kg of body weight). Tail venous blood glucose was monitored at 0, 15, 30, 60, 90 and 120 min after glucose administration. Insulin tolerance was performed on 5 h-fasted mice after an intraperitoneal injection of insulin (0.75 U/kg of body weight; Humulin® S; Lilly, UK). Tail venous blood glucose was monitored at 0, 15, 30, 60 min. *In vivo* glucose-stimulated insulin secretion was assessed after intraperitoneal injection of glucose (3 g/kg) and blood was collected at 0, 2.5, 5

and 15 post-injection. Plasma insulin levels were measured using a homogenous time-resolved fluorescence (HTRF) mouse insulin kit (Cisbio, France).

Isolation of mouse islets

Islets were isolated by digestion with collagenase as described (45). In brief, pancreata were inflated with a collagenase solution (1 mg/mL) and placed in a water bath at 37 ^{0}C for 12 min. After several washes, the islets were purified on a Histopaque gradient (Sigma-Aldrich, UK), and isolated islets were cultured 24 h in RPMI 1640 containing 11.1 mM glucose, 10% foetal bovine serum and L-glutamine (Sigma-Aldrich, UK) and allowed to recover overnight.

***Ex vivo* glucose-stimulated insulin secretion**

Insulin secretion assays on isolated mouse islets were performed as previously described (15). In brief, 10 size-matched islets per condition were incubated for 1h in Krebs-HEPES-bicarbonate (KHB) solution [in mM: 130 NaCl, 3.6 KCl, 1.5 $CaCl_2$, 0.5 $MgSO_4$, 0.5 KH_2PO_4, 2 $NaHCO_3$, 10 HEPES, and 0.1% (wt/vol) BSA, pH 7.4] containing 3 mM glucose. Subsequently, islets were incubated for 30 min. in KHB solution with either 3 mM glucose, 17 mM glucose or 30 mM KCl. Secreted and total insulin were quantified using a HTRF insulin kit (Cisbio, France) in a PHERAstar reader (BMG Labtech, UK) following the manufacturer's guidelines.

RNA extraction and quantitative real-time PCR analysis

RNA was isolated and purified from fresh isolated islets (50-200) with TRIzol reagent (Invitrogen, USA) according to the manufacturer's instructions. RNA purity and concentration were measured by spectrophotometry (Nanodrop, Thermofisher) and only RNA samples with an absorption ratio between 1.8-2.0 for 260/280 nm were used. cDNA was synthesized using 200 ng of RNA by the High-capacity cDNA Reverse Transcription kit (Applied Biosystems, USA) including random primers. For quantitative real-time PCR we used SYBR Green PCR master mix (Life Technologies, USA) and the primers sequences are in supplemental Table S2.

Immunohistochemistry and islet morphology

Isolated pancreata were removed from euthanized mice and fixed overnight in 10% (v/v) formalin and subsequently embedded in paraffin wax. Sections (5 μm) were cut and fixed in superfrost slides. Slides were prepared as detailed (25). For antigen retrieval before specific antigen detection, sections were treated with Tris-EDTA buffer, pH 9.0, at 95°C for 20 min. Primary antibodies used were anti-guinea pig insulin (1:200; Dako, USA), anti-mouse glucagon (1:1000; Sigma-Aldrich, UK), anti-E-cadherin (1:100; Cell Signaling Technology, USA), anti-Ki67 (1:200; Abcam, UK). Slides were visualized using an Axiovert 200 M microscope (Zeiss, Germany) with Alexa Fluor 488 goat anti-guinea pig IgG, Alexa Fluor 568 donkey anti-mouse IgG, Alexa Fluor 488 goat anti-rabbit IgG or Alexa Fluor 568 goat anti-guinea-pig IgG (Invitrogen, UK). ImageJ software (Wayne Rasband, National Institute of Mental Health) was used to calculate the β cell mass and size. We determined the percentage of pancreatic surface that was insulin or glucagon positive, as measured in 4 sections separated by 75 μm in the z-axis from six to seven mice of each genotype. For Ki-67 and E-cadherin detection, pancreata from three 10-week-old mice in each genotype were examined. At least three 5-μm sections per mouse at least 150 μm apart were analysed. To quantify the number of "rosette-like" structures (i.e., 8–10 cells arranged concentrically around an identifiable central "core") in islets (15), we used E-cadherin and DAPI staining of pancreatic sections. Structures were included where the void at the center was negative for DAPI. Ten islets per mouse and three mice per genotype were assessed.

Western (immuno-) blotting

After isolation, islets were collected and lysed in ice-cold buffer (150 mM NaCl, 10 mM Tris-HCl pH 7.2, 0.1% SDS, 1% deoxycholate, 5 mM EDTA, 1% Triton-

X100) containing protease inhibitor cocktail (Roche, UK) and phosphatase inhibitors (Sigma-Aldrich, UK). Lysates from 125 islets were denatured for 5 min. at 95^{0}C in Laemmli buffer, and resolved by 10% SDS-PAGE, and transferred to PVDF membranes before immunoblotting. Intensities were quantified using ImageJ.

Antibodies

Antibodies used in Western (immuno-)blot analysis and immunohistochemistry were the following: rabbit anti-phospho-S6 Ribosomal Protein (Ser235/236) (Cell signaling Technology, USA), mouse anti-α-tubulin (Sigma-Aldrich, UK), rabbit anti-E-cadherin (Cell signaling Technology, USA), guinea-pig anti-insulin (Dako, USA), mouse anti-glucagon (Sigma-Aldrich, UK), and rabbit anti-Ki67 (Abcam, UK).

Measurement of intracellular free calcium

Whole isolated islets were incubated with fura-8AM (Invitrogen) for 45 min at 37^{0}C in KHB containing 3 mmol/L glucose. Fluorescence imaging was performed using a Nipkow spinning disk head, allowing rapid scanning of islet areas for prolonged periods of time with minimal phototoxicity. Velocity software (PerkinElmer Life Sciences) provided interface while islets were kept at 37^{0}C and constantly perifused with KHB containing 3 mmol/L or 17 mmol/L glucose or 20 mmol/L KCl. For each experiment we used 16-29 islets. Imaging data were analysed with ImageJ software using an in-house macro (46).

Statistical analysis

GraphPad Prism 7.0 was used for statistical analysis. Statistical significance was evaluated by the two-tailed paired Student t test and one- or two-way ANOVA with a Bonferroni or Tukey post hoc test when appropriate. All data are shown as means ± SEM. P values of <0.05 were considered statistically significant.

Conflict of interest: The authors declare that they have no conflicts of interest with the contents of this article.

Reference List

1. Kahn, S. E., Zraika, S., Utzschneider, K. M., and Hull, R. L. (2009) The beta cell lesion in type 2 diabetes: there has to be a primary functional abnormality. *Diabetologia.* **52,** 1003-1012

2. Fuchsberger, C., Flannick, J., Teslovich, T. M., Mahajan, A., Agarwala, V., Gaulton, K. J., Ma, C., Fontanillas, P., Moutsianas, L., McCarthy, D. J., Rivas, M. A., Perry, J. R., Sim, X., Blackwell, T. W., Robertson, N. R., Rayner, N. W., Cingolani, P., Locke, A. E., Tajes, J. F., Highland, H. M., Dupuis, J., Chines, P. S., Lindgren, C. M., Hartl, C., Jackson, A. U., Chen, H., Huyghe, J. R., van de Bunt, M., Pearson, R. D., Kumar, A., Muller-Nurasyid, M., Grarup, N., Stringham, H. M., Gamazon, E. R., Lee, J., Chen, Y., Scott, R. A., Below, J. E., Chen, P., Huang, J., Go, M. J., Stitzel, M. L., Pasko, D., Parker, S. C., Varga, T. V., Green, T., Beer, N. L., Day-Williams, A. G., Ferreira, T., Fingerlin, T., Horikoshi, M., Hu, C., Huh, I., Ikram, M. K., Kim, B. J., Kim, Y., Kim, Y. J., Kwon, M. S., Lee, J., Lee, S., Lin, K. H., Maxwell, T. J., Nagai, Y., Wang, X., Welch, R. P., Yoon, J., Zhang, W., Barzilai, N., Voight, B. F., Han, B. G., Jenkinson, C. P., Kuulasmaa, T., Kuusisto, J., Manning, A., Ng, M. C., Palmer, N. D., Balkau, B., Stancakova, A., Abboud, H. E., Boeing, H., Giedraitis, V., Prabhakaran, D., Gottesman, O., Scott, J., Carey, J., Kwan, P., Grant, G., Smith, J. D., Neale, B. M., Purcell, S., Butterworth, A. S., Howson, J. M., Lee, H. M., Lu, Y., Kwak, S. H., Zhao, W., Danesh, J., Lam, V. K., Park, K. S., Saleheen, D., So, W. Y., Tam, C. H., Afzal, U., Aguilar, D., Arya, R., Aung, T., Chan, E., Navarro, C., Cheng, C. Y., Palli, D., Correa, A., Curran, J. E., Rybin, D., Farook, V. S., Fowler, S. P., Freedman, B. I., Griswold, M., Hale, D. E., Hicks, P. J., Khor, C. C., Kumar, S., Lehne, B., Thuillier, D., Lim, W. Y., Liu, J., van der Schouw, Y. T., Loh, M., Musani, S. K., Puppala, S., Scott, W. R., Yengo, L., Tan, S. T., Taylor, H. A., Jr., Thameem, F., Wilson, G., Wong, T. Y., Njolstad, P. R., Levy, J. C., Mangino, M., Bonnycastle, L. L., Schwarzmayr, T., Fadista, J., Surdulescu, G. L., Herder, C., Groves, C. J., Wieland, T., Bork-Jensen, J., Brandslund, I., Christensen, C., Koistinen, H. A., Doney, A. S., Kinnunen, L., Esko, T., Farmer, A. J., Hakaste, L., Hodgkiss, D., Kravic, J., Lyssenko, V., Hollensted, M., Jorgensen, M. E., Jorgensen, T., Ladenvall, C., Justesen, J. M., Karajamaki, A., Kriebel, J., Rathmann, W., Lannfelt, L., Lauritzen, T., Narisu, N., Linneberg, A., Melander, O., Milani, L., Neville, M., Orho-Melander, M., Qi, L., Qi, Q., Roden, M., Rolandsson, O., Swift, A., Rosengren, A. H., Stirrups, K., Wood, A. R., Mihailov, E., Blancher, C., Carneiro, M. O., Maguire, J., Poplin, R., Shakir, K., Fennell, T., DePristo, M., Hrabe de, A. M., Deloukas, P., Gjesing, A. P., Jun, G., Nilsson, P., Murphy, J., Onofrio, R., Thorand, B., Hansen, T., Meisinger, C., Hu, F. B., Isomaa, B., Karpe, F., Liang, L., Peters, A., Huth, C., O'Rahilly, S. P., Palmer, C. N., Pedersen, O., Rauramaa, R., Tuomilehto, J., Salomaa, V., Watanabe, R. M., Syvanen, A. C., Bergman, R. N., Bharadwaj, D., Bottinger, E. P., Cho, Y. S., Chandak, G. R., Chan, J. C., Chia, K. S., Daly, M. J., Ebrahim, S. B., Langenberg, C., Elliott, P., Jablonski, K. A., Lehman, D. M., Jia, W., Ma, R. C., Pollin, T. I., Sandhu, M., Tandon, N., Froguel, P., Barroso, I., Teo, Y. Y., Zeggini, E., Loos, R. J., Small, K. S., Ried, J. S., DeFronzo, R. A., Grallert, H., Glaser, B., Metspalu, A., Wareham, N. J., Walker, M., Banks, E., Gieger, C., Ingelsson, E., Im, H. K., Illig, T., Franks, P. W., Buck, G., Trakalo, J., Buck, D., and Prokopenko, I. (2016) The genetic architecture of type 2 diabetes. *Nature.* **536,** 41-47

3. van de Bunt, M., Manning Fox, J. E., Dai, X., Barrett, A., Grey, C., Li, L., Bennett, A. J., Johnson, P. R., Rajotte, R. V., Gaulton, K. J., Dermitzakis, E. T., MacDonald, P. E., McCarthy, M. I., and Gloyn, A. L. (2015) Transcript Expression Data from Human Islets Links Regulatory Signals from Genome-Wide Association Studies for Type 2 Diabetes and Glycemic Traits to Their Downstream Effectors. *PLoS. Genet.* **11,** e1005694

4. Mehta, Z. B., Fine, N., Pullen, T. J., Cane, M. C., Hu, M., Chabosseau, P., Meur, G., Velayos-Baeza, A., Monaco, A. P., Marselli, L., Marchetti, P., and Rutter, G. A. (2016) Changes in the expression of the type 2 diabetes-associated gene VPS13C in the beta cell are associated with glucose intolerance in humans and mice. *Am. J. Physiol Endocrinol. Metab.* **311,** E488-E507

5. Grant, S. F., Thorleifsson, G., Reynisdottir, I., Benediktsson, R., Manolescu, A., Sainz, J., Helgason, A., Stefansson, H., Emilsson, V., Helgadottir, A., Styrkarsdottir, U., Magnusson, K. P., Walters, G. B., Palsdottir, E., Jonsdottir, T., Gudmundsdottir, T., Gylfason, A., Saemundsdottir, J., Wilensky, R. L., Reilly, M. P., Rader, D. J., Bagger, Y., Christiansen, C., Gudnason, V., Sigurdsson, G., Thorsteinsdottir, U., Gulcher, J. R., Kong, A., and Stefansson, K. (2006) Variant of transcription factor 7-like 2 (TCF7L2) gene confers risk of type 2 diabetes. *Nat. Genet.* **38,** 320-323

6. Zeggini, E. and McCarthy, M. I. (2007) TCF7L2: the biggest story in diabetes genetics since HLA? *Diabetologia.* **50,** 1-4

7. Brantjes, H., Barker, N., van, E. J., and Clevers, H. (2002) TCF: Lady Justice casting the final verdict on the outcome of Wnt signalling. *Biol. Chem.* **383,** 255-261

8. Habener, J. F. and Liu, Z. (2014) Wnt signalling in pancreatic islets. In Islam, M., editor. *Islets of Langerhans,* Springer, Dordecht

9. da Silva Xavier, G., Loder, M. K., McDonald, A., Tarasov, A. I., Carzaniga, R., Kronenberger, K., Barg, S., and Rutter, G. A. (2009) TCF7L2 regulates late events in insulin secretion from pancreatic islet beta-cells. *Diabetes* **58,** 894-905

10. Zhou, Y., Park, S. Y., Su, J., Bailey, K., Ottosson-Laakso, E., Shcherbina, L., Oskolkov, N., Zhang, E., Thevenin, T., Fadista, J., Bennet, H., Vikman, P., Wierup, N., Fex, M., Rung, J., Wollheim, C., Nobrega, M., Renstrom, E., Groop, L., and Hansson, O. (2014) TCF7L2 is a master regulator of insulin production and processing. *Hum. Mol. Genet.* **23,** 6419-6431

11. da Silva Xavier, G., Mondragon, A., Sun, G., Chen, L., McGinty, J. A., French, P. M., and Rutter, G. A. (2012) Abnormal glucose tolerance and insulin secretion in pancreas-specific Tcf7l2 null mice. *Diabetologia* **55,** 2667-2676

12. Mitchell, R. K., Mondragon, A., Chen, L., McGinty, J. A., French, P. M., Ferrer, J., Thorens, B., Hodson, D. J., Rutter, G. A., and da Silva Xavier, G. (2014) Selective disruption of Tcf7l2 in the pancreatic beta cell impairs secretory function and lowers beta cell mass. *Hum Mol Genet* **24,** 1390-1399

13. Savic, D., Ye, H., Aneas, I., Park, S. Y., Bell, G. I., and Nobrega, M. A. (2011) Alterations in TCF7L2 expression define its role as a key regulator of glucose metabolism. *Genome Res.* **21,** 1417-1425

14. Ahlqvist, E., Storm, P., Karajamaki, A., Martinell, M., Dorkhan, M., Carlsson, A., Vikman, P., Prasad, R. B., Aly, D. M., Almgren, P., Wessman, Y., Shaat, N., Spegel, P., Mulder, H., Lindholm, E., Melander, O., Hansson, O., Malmqvist, U., Lernmark, A., Lahti, K., Forsen, T., Tuomi, T., Rosengren, A. H., and Groop, L. (2018) Novel subgroups of adult-onset diabetes and their association with outcomes: a data-driven cluster analysis of six variables. *Lancet Diabetes Endocrinol.* **6,** 361-369

15. Sun, G., Tarasov, A. I., McGinty, J. A., French, P. M., McDonald, A., Leclerc, I., and Rutter, G. A. (2010) LKB1 deletion with the RIP.Cre-transgene modifies pancreatic {beta}-cell morphology and enhances insulin secretion in vivo. *Am. J. Physiol Endocrinol. Metab.* **298,** E1261-E1273

16. Swisa, A., Granot, Z., Tamarina, N., Sayers, S., Bardeesy, N., Philipson, L., Hodson, D. J., Wikstrom, J. D., Rutter, G. A., Leibowitz, G., Glaser, B., and Dor, Y. (2015) Loss of Liver Kinase B1 (LKB1) in Beta Cells Enhances Glucose-stimulated Insulin Secretion Despite Profound Mitochondrial Defects. *J. Biol. Chem.* **290,** 20934-20946

17. Fu, A., Ng, A. C., Depatie, C., Wijesekara, N., He, Y., Wang, G. S., Bardeesy, N., Scott, F. W., Touyz, R. M., Wheeler, M. B., and Screaton, R. A. (2009) Loss of Lkb1 in adult beta cells increases beta cell mass and enhances glucose tolerance in mice. *Cell Metab.* **10,** 285-295

18. Granot, Z., Swisa, A., Magenheim, J., Stolovich-Rain, M., Fujimoto, W., Manduchi, E., Miki, T., Lennerz, J. K., Stoeckert, C. J., Jr., Meyuhas, O., Seino, S., Permutt, M. A., Piwnica-Worms, H., Bardeesy, N., and Dor, Y. (2009) LKB1 regulates pancreatic beta cell size, polarity, and function. *Cell Metab.* **10,** 296-308

19. Boardman, L. A., Thibodeau, S. N., Schaid, D. J., Lindor, N. M., McDonnell, S. K., Burgart, L. J., Ahlquist, D. A., Podratz, K. C., Pittelkow, M., and Hartmann, L. C. (1998) Increased risk for cancer in patients with the Peutz-Jeghers syndrome. *Ann. Intern. Med.* **128,** 896-899

20. Jenne, D. E., Reimann, H., Nezu, J., Friedel, W., Loff, S., Jeschke, R., Muller, O., Back, W., and Zimmer, M. (1998) Peutz-Jeghers syndrome is caused by mutations in a novel serine threonine kinase. *Nat. Genet.* **18,** 38-43

21. Fu, A., Robitaille, K., Faubert, B., Reeks, C., Dai, X. Q., Hardy, A. B., Sankar, K. S., Ogrel, S., Al-Dirbashi, O. Y., Rocheleau, J. V., Wheeler, M. B., MacDonald, P. E., Jones, R., and Screaton, R. A. (2015) LKB1 couples glucose metabolism to insulin secretion in mice. *Diabetologia.* **58,** 1513-1522

22. Inoki, K., Zhu, T., and Guan, K. L. (2003) TSC2 mediates cellular energy response to control cell growth and survival. *Cell* **115,** 577-590

23. Salt, I. P., Johnson, G., Ashcroft, S. J., and Hardie, D. G. (1998) AMP-activated protein kinase is activated by low glucose in cell lines derived from pancreatic beta cells, and may regulate insulin release. *Biochem J* **335,** 533-539

24. daSilvaXavier, G., Leclerc, I., Varadi, A., Tsuboi, T., Moule, S. K., and Rutter, G. A. (2003) Role for AMP-activated protein kinase in glucose-stimulated insulin secretion and preproinsulin gene expression. *Biochem. J.* **371,** 761-774

25. Kone, M., Pullen, T. J., Sun, G., Ibberson, M., Martinez-Sanchez, A., Sayers, S., Nguyen-Tu, M. S., Kantor, C., Swisa, A., Dor, Y., Gorman, T., Ferrer, J., Thorens, B., Reimann, F., Gribble, F., McGinty, J. A., Chen, L., French, P. M., Birzele, F., Hildebrandt, T., Uphues, I., and Rutter, G. A. (2014) LKB1 and AMPK differentially regulate pancreatic beta-cell identity. *FASEB J.* **28,** 4972-4985

26. Thorens, B., Tarussio, D., Maestro, M. A., Rovira, M., Heikkila, E., and Ferrer, J. (2015) Ins1 knock-in mice for beta cell-specific gene recombination. *Diabetologia* **58,** 558-656

27. Brouwers, B., de, F. G., Osipovich, A. B., Goyvaerts, L., Lemaire, K., Boesmans, L., Cauwelier, E. J., Granvik, M., Pruniau, V. P., Van, L. L., Van, S. J., Stancill, J. S., Smolders, I., Goffin, V., Binart, N., in't, V. P., Declercq, J., Magnuson, M. A., Creemers, J. W., Schuit, F., and Schraenen, A. (2014) Impaired islet function in commonly used transgenic mouse lines due to human growth hormone minigene expression. *Cell Metab.* **20,** 979-990

28. Bouwens, L. and Rooman, I. (2005) Regulation of pancreatic beta-cell mass. *Physiol Rev.* **85,** 1255-1270

29. Ackermann, A. M. and Gannon, M. (2007) Molecular regulation of pancreatic beta-cell mass development, maintenance, and expansion. *J. Mol Endocrinol.* **38,** 193-206

30. Rieck, S. and Kaestner, K. H. (2010) Expansion of beta-cell mass in response to pregnancy. *Trends Endocrinol. Metab.* **21,** 151-158

31. Butler, A. E., Cao-Minh, L., Galasso, R., Rizza, R. A., Corradin, A., Cobelli, C., and Butler, P. C. (2010) Adaptive changes in pancreatic beta cell fractional area and beta cell turnover in human pregnancy. *Diabetologia.* **53,** 2167-2176

32. Sachdeva, M. M. and Stoffers, D. A. (2009) Minireview: Meeting the demand for insulin: molecular mechanisms of adaptive postnatal beta-cell mass expansion. *Mol Endocrinol.* **23,** 747-758

33. Mezza, T., Muscogiuri, G., Sorice, G. P., Clemente, G., Hu, J., Pontecorvi, A., Holst, J. J., Giaccari, A., and Kulkarni, R. N. (2014) Insulin resistance alters islet morphology in nondiabetic humans. *Diabetes.* **63,** 994-1007

34. Pound, L. D., Sarkar, S. A., Benninger, R. K., Wang, Y., Suwanichkul, A., Shadoan, M. K., Printz, R. L., Oeser, J. K., Lee, C. E., Piston, D. W., McGuinness, O. P., Hutton, J. C., Powell, D. R., and O'Brien, R. M. (2009) Deletion of the mouse Slc30a8 gene encoding zinc transporter-8 results in impaired insulin secretion. *Biochem. J.* **421,** 371-376

35. Nicolson, T. J., Bellomo, E. A., Wijesekara, N., Loder, M. K., Baldwin, J. M., Gyulkhandanyan, A. V., Koshkin, V., Tarasov, A. I., Carzaniga, R., Kronenberger, K., Taneja, T. K., da, S., X, Libert, S., Froguel, P., Scharfmann, R., Stetsyuk, V., Ravassard, P., Parker, H., Gribble, F. M., Reimann, F., Sladek, R., Hughes, S. J.,

Johnson, P. R., Masseboeuf, M., Burcelin, R., Baldwin, S. A., Liu, M., Lara-Lemus, R., Arvan, P., Schuit, F. C., Wheeler, M. B., Chimienti, F., and Rutter, G. A. (2009) Insulin storage and glucose homeostasis in mice null for the granule zinc transporter ZnT8 and studies of the type 2 diabetes-associated variants. *Diabetes* **58,** 2070-2083

36. Rutter, G. A. and Chimienti, F. (2015) SLC30A8 mutations in type 2 diabetes. *Diabetologia* **58,** 31-36

37. Muncan, V., Faro, A., Haramis, A. P., Hurlstone, A. F., Wienholds, E., van, E. J., Korving, J., Begthel, H., Zivkovic, D., and Clevers, H. (2007) T-cell factor 4 (Tcf7l2) maintains proliferative compartments in zebrafish intestine. *EMBO Rep.* **8,** 966-973

38. Clevers, H. (2006) Wnt/beta-catenin signaling in development and disease. *Cell.* **127,** 469-480

39. Montgomery, M. K., Hallahan, N. L., Brown, S. H., Liu, M., Mitchell, T. W., Cooney, G. J., and Turner, N. (2013) Mouse strain-dependent variation in obesity and glucose homeostasis in response to high-fat feeding. *Diabetologia.* **56,** 1129-1139

40. Cruciani-Guglielmacci, C., Bellini, L., Denom, J., Oshima, M., Fernandez, N., Normandie-Levi, P., Berney, X. P., Kassis, N., Rouch, C., Dairou, J., Gorman, T., Smith, D. M., Marley, A., Liechti, R., Kuznetsov, D., Wigger, L., Burdet, F., Lefevre, A. L., Wehrle, I., Uphues, I., Hildebrandt, T., Rust, W., Bernard, C., Ktorza, A., Rutter, G. A., Scharfmann, R., Xenarios, I., Le, S. H., Thorens, B., Magnan, C., and Ibberson, M. (2017) Molecular phenotyping of multiple mouse strains under metabolic challenge uncovers a role for Elovl2 in glucose-induced insulin secretion. *Mol Metab.* **6,** 340-351

41. Henquin, J. C. (2000) Triggering and amplifying pathways of regulation of insulin secretion by glucose. *Diabetes* **49,** 1751-1760

42. Rutter, G. A., Pullen, T. J., Hodson, D. J., and Martinez-Sanchez, A. (2015) Pancreatic beta cell identity, glucose sensing and the control of insulin secretion. *Biochem. J.* **466,** 202-218

43. Ashcroft, F. M. and Rorsman, P. (2013) K(ATP) channels and islet hormone secretion: new insights and controversies. *Nat. Rev. Endocrinol.* **9,** 660-669

44. Heni, M., Ketterer, C., Thamer, C., Herzberg-Schafer, S. A., Guthoff, M., Stefan, N., Machicao, F., Staiger, H., Fritsche, A., and Haring, H. U. (2010) Glycemia determines the effect of type 2 diabetes risk genes on insulin secretion. *Diabetes.* **59,** 3247-3252

45. Ravier, M. A. and Rutter, G. A. (2010) Isolation and culture of mouse pancreatic islets for ex vivo imaging studies with trappable or recombinant fluorescent probes. *Methods Mol. Biol.* **633,** 171-184

46. Mitchell, R. K., Nguyen-Tu, M. S., Chabosseau, P., Callingham, R. M., Pullen, T. J., Cheung, R., Leclerc, I., Hodson, D. J., and Rutter, G. A. (2017) The transcription factor Pax6 is required for pancreatic beta cell identity, glucose-regulated ATP synthesis, and Ca2+ dynamics in adult mice. *J. Biol. Chem.* **292,** 8892-8906

FOOTNOTES

Funding was provided by MRC Programme (MR/J0003042/1; MR/N00275X/1; MR/L020149/1 [DIVA]), Wellcome Trust Senior Investigator (WT098424AIA) and Royal Society Wolfson Research Merit Awards, and Diabetes UK Project (BDA11/0004210; BDA/15/0005275) grants to G.A.R.

The abbreviations used are: AMPK, AMP-activated protein kinase; GSK-3β, glycogen synthase kinase 3β; GWAS, Genome-wide association studies; LKB1, liver kinase B1; mTOR, mammalian target of rapamycin; TCF7L2, transcription factor-7-like 2; TSC1/TSC2; Tuberous Sclerosis Complex

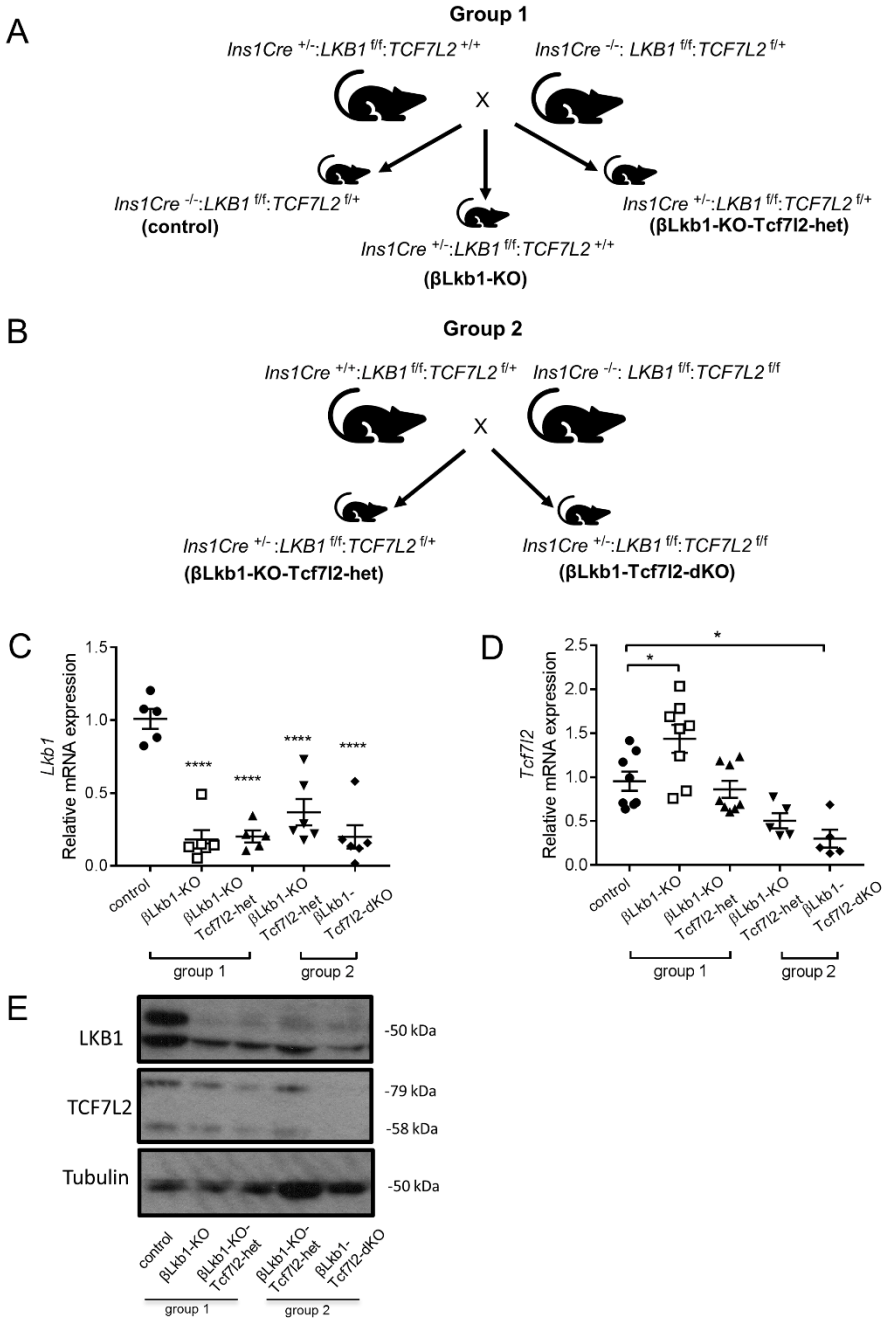

Figure 1: Breeding strategy for the generation of *Lkb1/Tcf7l2* deletion mutants in the β cell and confirmation of the mouse model. A: Littermate pups from group 1 display 3 different genotypes: control as Ins1Cre $^{-/-}$: Lkb1 $^{f/f}$: Tcf7l2 $^{f/+}$, Lkb1 deletion only as βLkb1-KO (Ins1Cre $^{+/-}$: Lkb1 $^{f/f}$: Tcf7l2 $^{+/+}$), and one single Tcf7l2 allele deleted in Lkb1 null background as βLkb1-KO-Tcf7l2-het (Ins1Cre $^{+/-}$: Lkb1 $^{f/f}$: Tcf7l2 $^{f/+}$). B: Littermate pups from group 2 display two different genotypes; one single Tcf7l2 allele deleted in a Lkb1 null background as βLkb1-KO-Tcf7l2-het (Ins1Cre $^{+/-}$: Lkb1 $^{f/f}$: Tcf7l2 $^{f/+}$) and two single Tcf7l2 alleles deleted in Lkb1 null background as βLkb1-Tcf7l2-dKO (Ins1Cre $^{+/-}$: Lkb1 $^{f/f}$: Tcf7l2 $^{f/f}$). C: RT-qPCR expression of Lkb1 mRNA in isolated islets (n=5-6 mice/genotype). D: RT-qPCR expression of Tcf7l2 mRNA in isolated islets (n=5-9 mice/genotype). E: Western blotting for TCF7L2 and LKB1 in isolated islets (n=2 mice/genotype). Error bars represent the mean of ± S.E.; *p<0.05, ****p<0.0001.

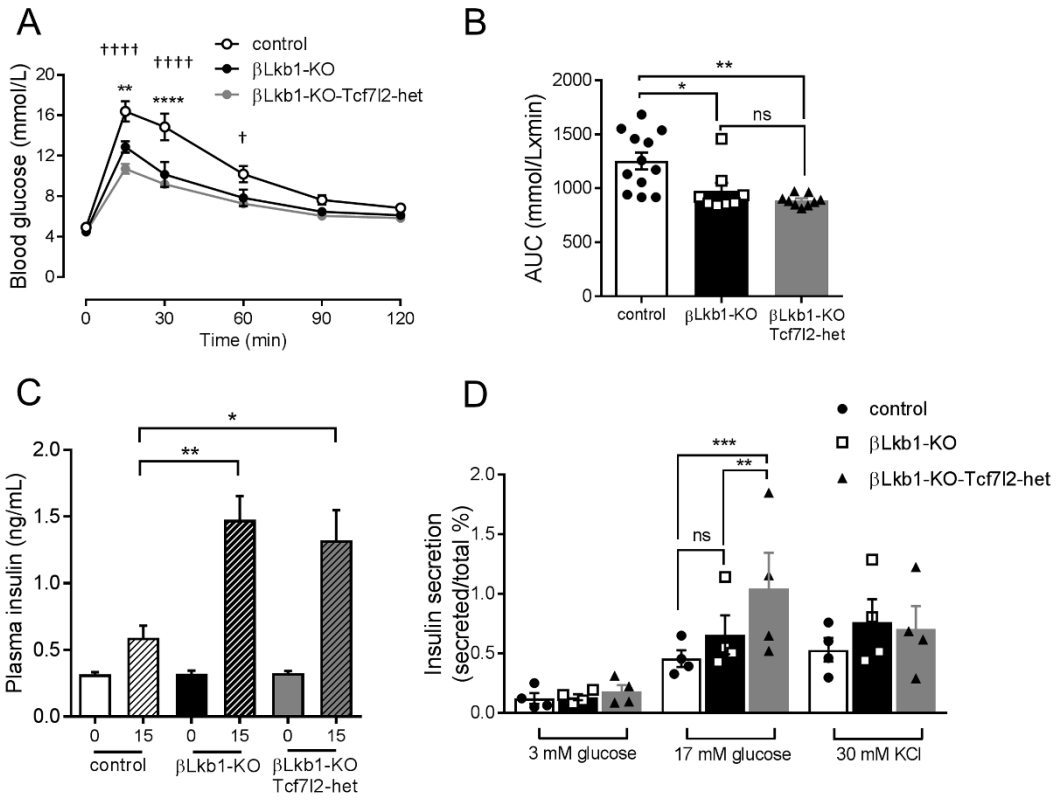

Figure 2: Monoallelic deletion does not affect *Lkb1* deletion-mediated improvements in glucose tolerance and augmented insulin secretion in males.

A: Oral glucose (2 g/kg) tolerance measurements were performed as described under Materials and Methods. n=9-12 mice/genotype; P value was statistically determined by a two-way ANOVA test with a Bonferroni post-test. **p<0.01, ****p<0.0001 βLkb1-KO vs control; †p< 0.05, ††††p<0.0001 βLkb1-KO-Tcf7l2-het vs control; p=0.623 βLkb1-KO vs βLkb1-KO-Tcf7l2-het. B: Area under the curve (AUC) for oral glucose tolerance tests (*p<0.05 βLkb1-KO vs control, **p<0.01 βLkb1-KO-Tcf7l2-het vs control).C: Insulin plasma levels were measured *in vivo* 15 minutes after intraperitoneal injection of glucose (3 g/kg) (n=7-9 mice/genotype; *p<0.05, **p<0.01 vs 15min-control. D: Insulin secretion *in vitro* was measured from groups of 10 size-matched isolated islets during static incubation (Research design and Methods) and at the indicated glucose or KCl concentrations (n=4 independent experiments; **p<0.01 βLkb1-KO-Tcf7l2-het vs βLkb1-KO, ***p<0.001 βLkb1-KO-Tcf7l2-het vs control); Error bars represent the mean of ± S.E.; ns=not significant.

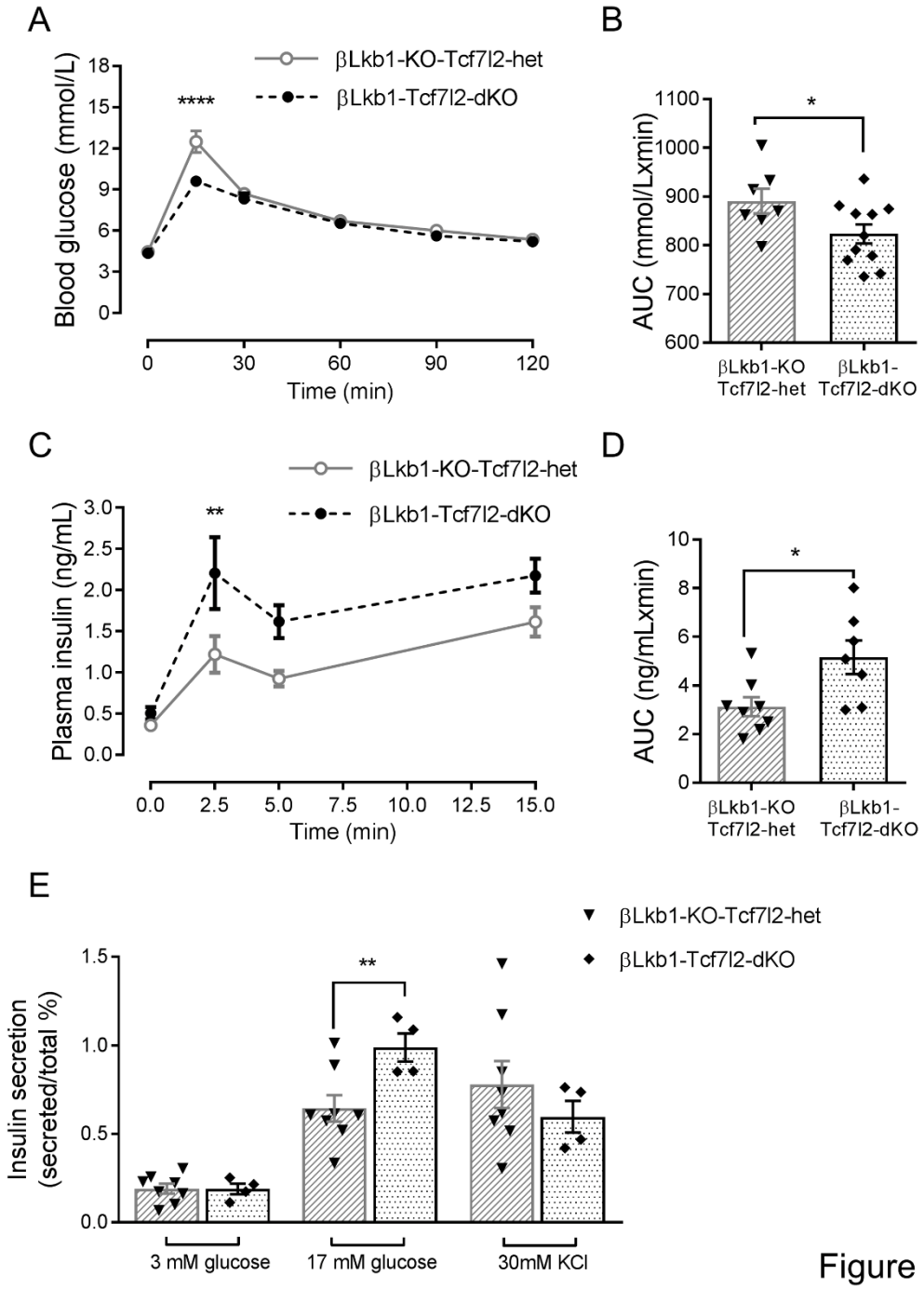

Figure 3: Deletion of both Tcf7l2 alleles potentiates the effects of *Lkb1* deletion on glucose tolerance and insulin secretion in males.

Experiments were performed as described in the legends to Figure 2 (A, B) oral glucose tolerance n=7-11 mice/genotype. Insulin plasma levels were measured *in vivo* 2.5, 5 and 15 minutes after intraperitoneal injection of glucose (3 g/kg) (C, D) n=7-8 mice/genotype, E: Insulin secretion *in vitro* was measured from groups of 10 size-matched isolated islets during static incubation (Research design and Methods) and at the indicated glucose or KCl concentrations; n=4-6 mice/genotype; *p<0.05, **p<0.01, ****p<0.0001. Grey open circle as βLkb1-KO-Tcf7l2-het, black circle as βLkb1-Tcf7l2-dKO; Error bars represent the mean of ± S.E.

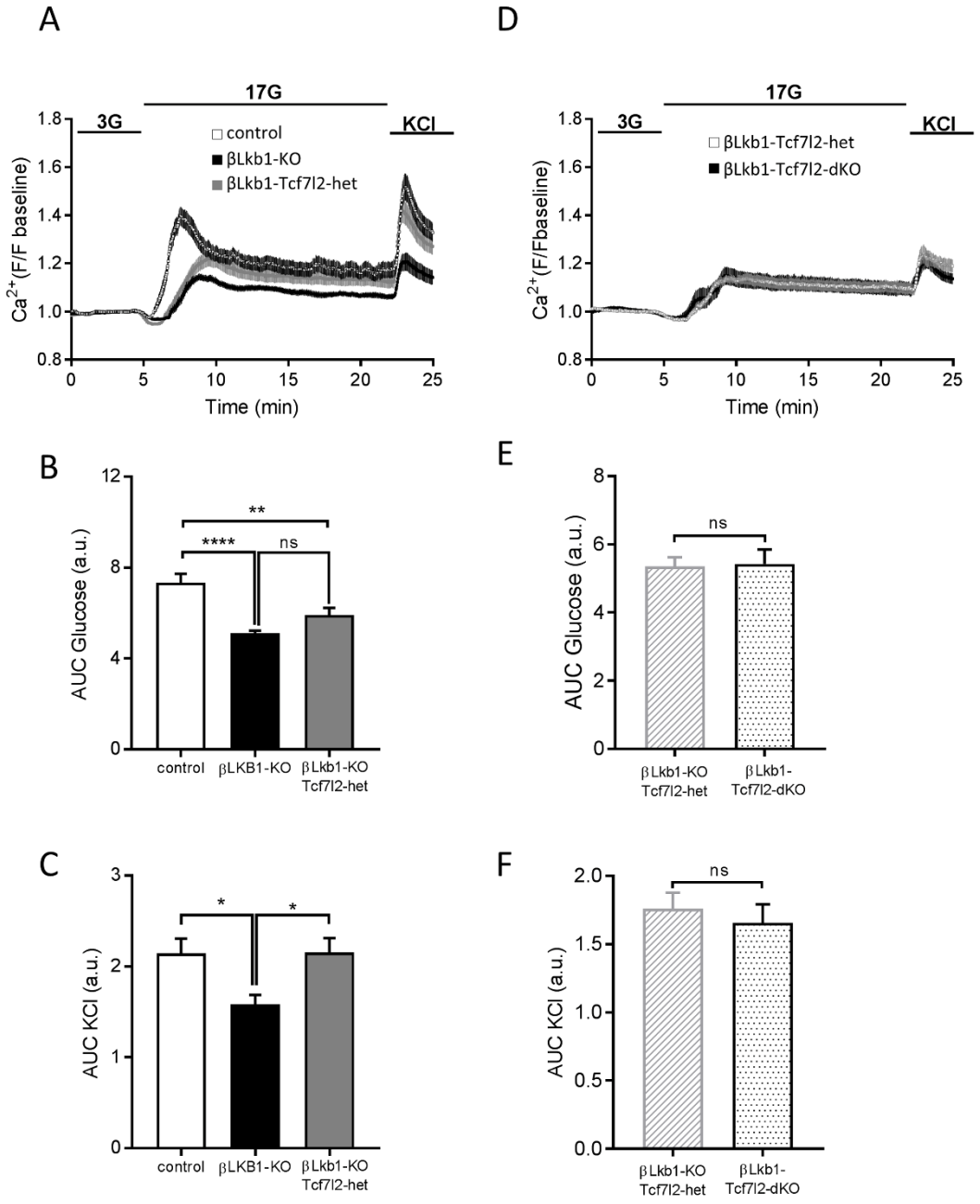

Figure 4

Figure 4: Deletion of one or two *Tcf7l2* alleles did not further alter Ca^{2+} dynamics in response to glucose but restored responses to KCl in males. A: Changes in free cytosolic Ca^{2+} in response to 3 mmol/L glucose (3G), 17 mmol/L glucose (17G) and 20 mmol/L KCl in group 1. B: Quantification of area under the curve for glucose responses. C: Quantification of area under the curve for KCl responses. D: Free cytosolic Ca^{2+} changes in response to 3 mmol/L glucose (3G), 17 mmol/L glucose (17G) and 20 mmol/L KCl in group 2. E: Quantification of area under the curve for glucose responses. F: Quantification of area under the curve for KCl responses. Each plot represents the average of 16-29 islets, n=3 per genotype. *p<0.05, **p<0.01, ****<p0.0001; Error bars represent the mean of ± S.E.; ns=not significant.

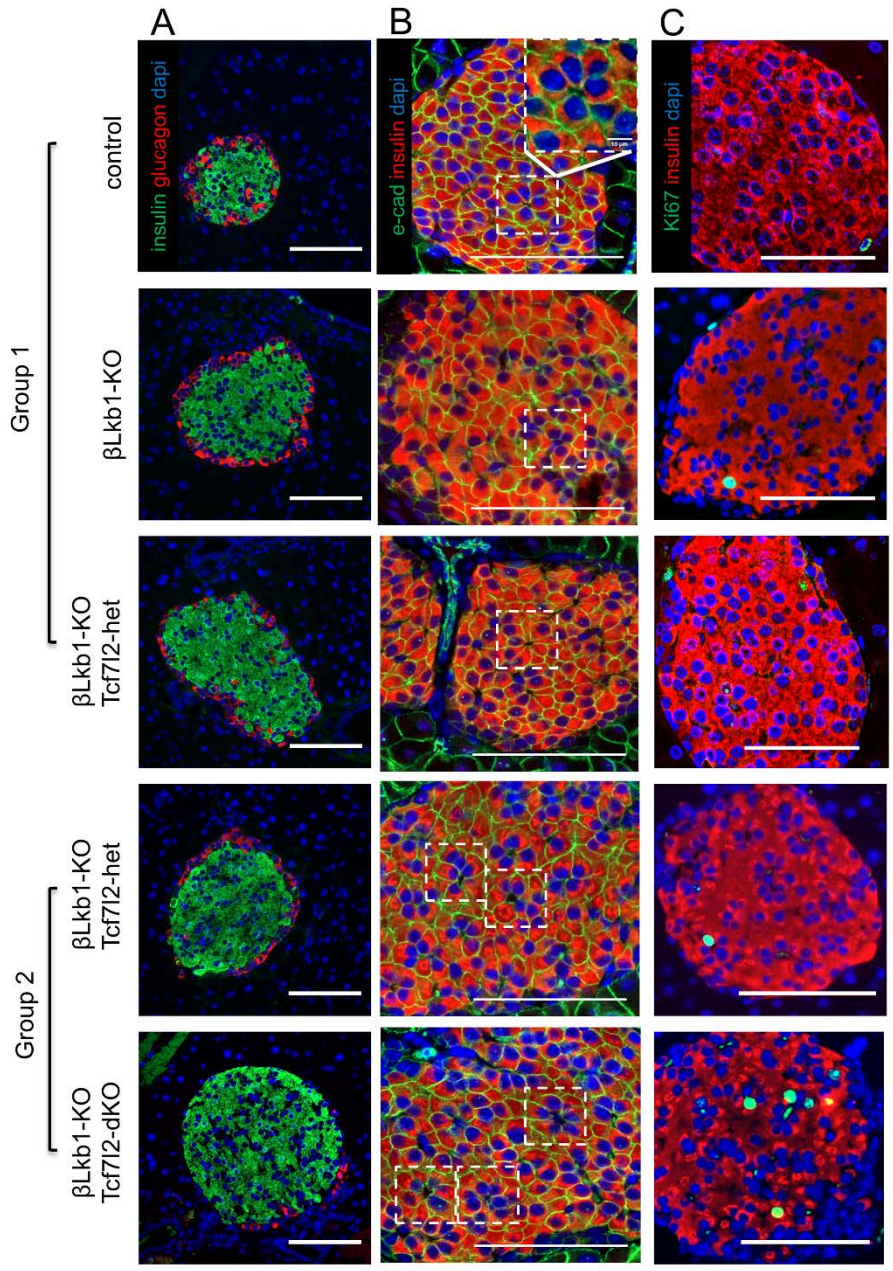

Figure 5

Figure 5: Impact of *Lkb1* or *Tcf7l2* deletion on islet topography in males. Representative immunohistochemistry results of pancreatic sections stained for β cell mass (A: insulin, 1:200, green; glucagon, 1:1000, red), for an adherens junction marker (B: E-cadherin, 1:100, green) and for a proliferation marker (C: Ki-67, 1:100, green). Rosette-like structure are localized in the white dotted line square and a representative image of a rosette-like structure is zoomed in column B in control mouse. Scale bar 100 μm.

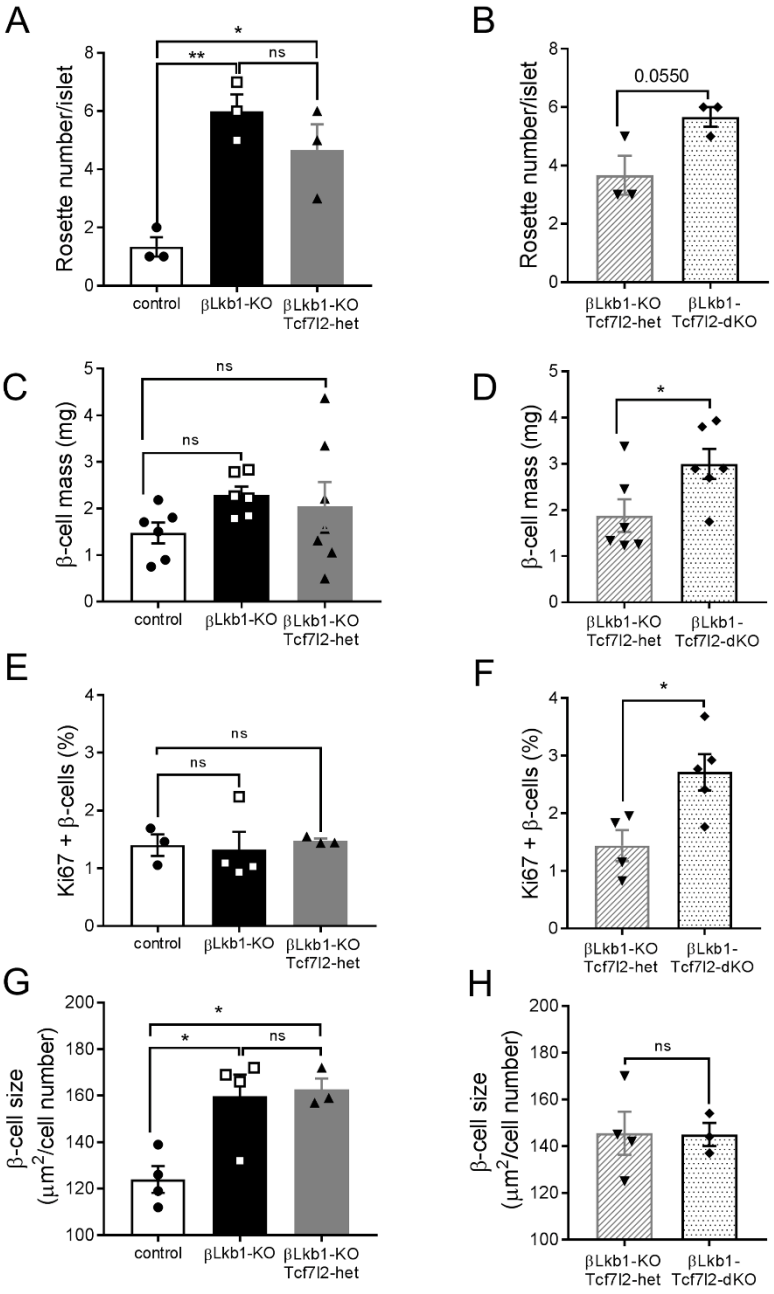

Figure 6

Figure 6: Effects of *Lkb1* or *Tcf7l2* deletion on β cell size and mass in males.
A, B: Rosette-like structure count per islet; n=3 mice/genotype in the group 1 (A) and in group 2 (B). C, D: β cell mass is the ratio of insulin positive staining to the total pancreatic surface and pancreas weight, n=6-7 mice/genotype. E, F: Quantification of Ki67 positive and insulin positive cells, based on 10-15 islets per pancreas; n=3-4 mice/genotype. G, H: Mean β cell size measured as the ratio of the insulin positive staining surface area to the number of β cells (n=3-4 mice/genotype) in the group 1 (G) and in group 2 (H). *p<0.05 **p<0.01. White bars as control, black bars as βLkb1-KO, grey bars as βLkb1-KO-Tcf7l2-het (group 1), hatched grey bars as βLkb1-KO-Tcf7l2-het (group 2) and dots black bars as βLkb1-Tcf7l2-dKO; Error bars represent the mean of ± S.E.; ns=not significant.

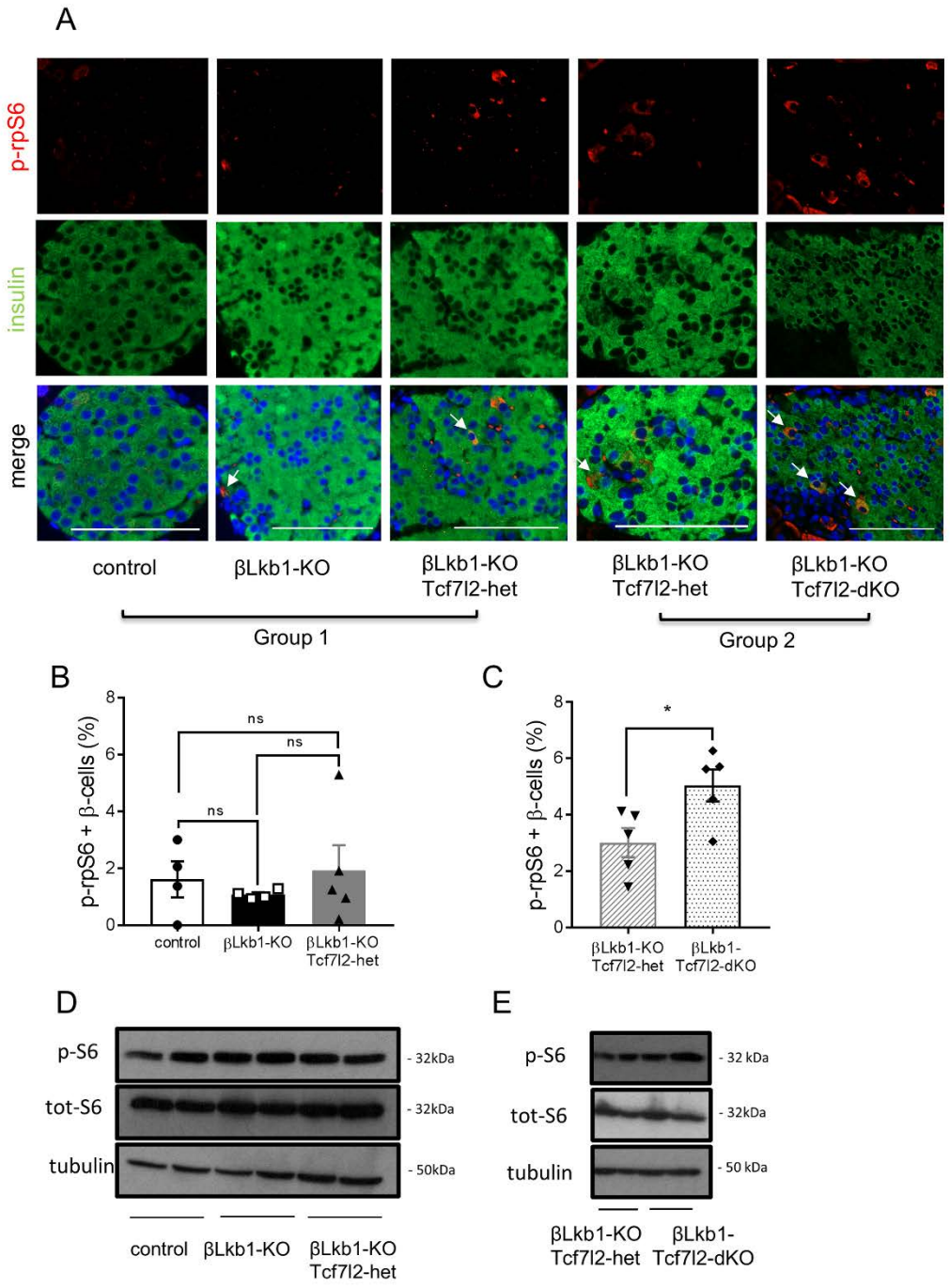

Figure 7: Deletion of *Tcf7l2* increases mTOR activity in *Lkb1* null islets from males.
A: Representative immunofluorescence staining of pancreatic sections from random-fed 10-week-old males using rabbit anti-phospho-ribosomal protein S6 (Ser235/236) (P-rpS6; 1:100; red) and guinea-pig anti-insulin antibodies (1:200; red). White arrows represent p-rpS6 and insulin colocalization. Scale bar, 100 µm. B/C: Quantification of p-rpS6 positive staining of total β cells per islet, based on 15-20 islets per pancreas from n=4-5 mice/genotype. White bars as control, black bars as βLkb1-KO grey bars as βLkb1-KO-Tcf7l2-het (B), hatched grey bars as βLkb1-KO-Tcf7l2-het (C) and dots black bars as βLkb1-Tcf7l2-dKO. D/E: Mouse pancreatic islets were isolated from animals of group 1 (D) and group 2 (E). After an overnight incubation in 11 mmol/L of glucose in RPMI media, isolated islets were collected and lysates from 125 islets were analysed by immunoblotting with anti-

phosphorylated (p-S6) and total (tot-S6) ribosomal protein-S6 (Ser235/236) and anti-tubulin for group 1 (D) and group 2 (E). Error bars represent the mean of ± S.E.; *p<0.05; ns=not significant.

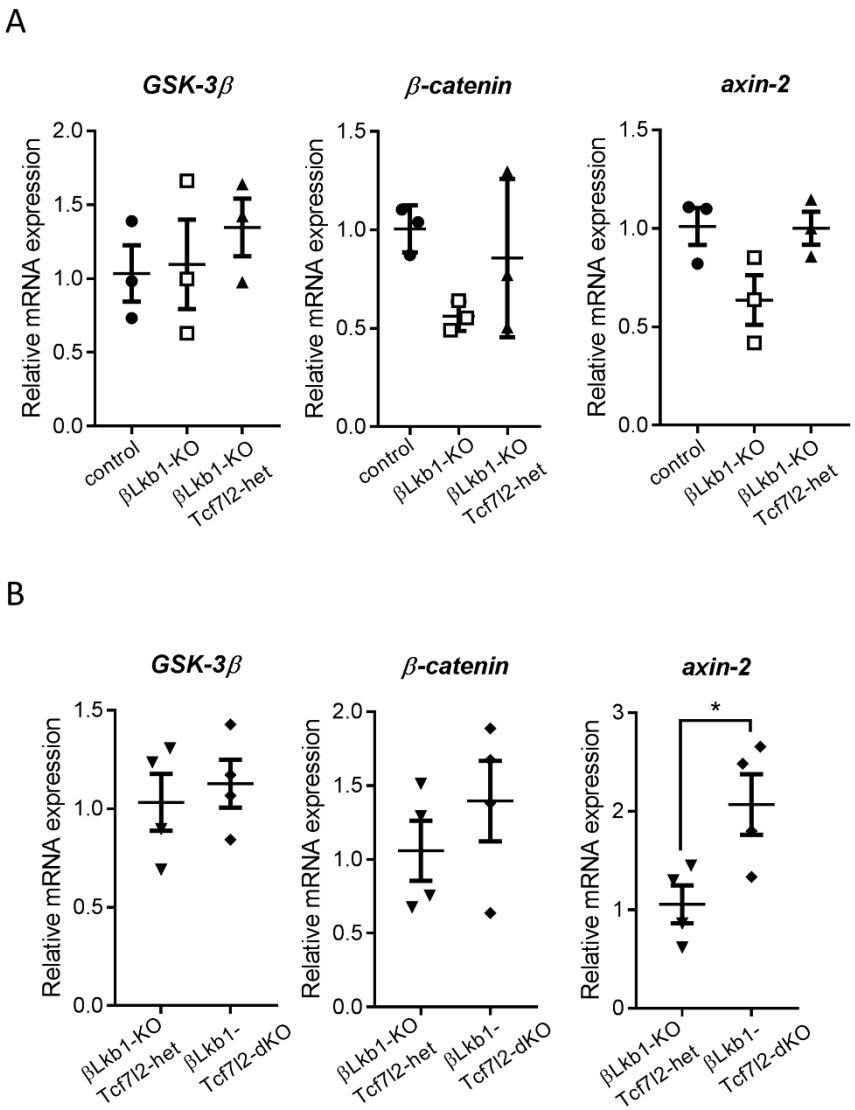

Figure 8: Wnt signalling is partly dependent on LKB1 and TCF7L2 in males. Wnt signalling target genes (GSK-3β, β-catenin and axin-2) expression was assessed by RT-qPCR in isolated islets from group 1 (A) and group 2 (B); n=2-3 mice/genotype. Error bars represent the mean of ± S.E.; *p<0.05.